AFRL-SN-RS-TR-2007-102
Final Technical Report
April 2007

NON-ELECTRONIC RADIO FRONT-END (NERF)

University of California

Sponsored by
Defense Advanced Research Projects Agency
DARPA Order No. N584/05

AIR FORCE RESEARCH LABORATORY
SENSORS DIRECTORATE
ROME RESEARCH SITE
ROME, NEW YORK

NOTICE AND SIGNATURE PAGE

Using Government drawings, specifications, or other data included in this document for any purpose other than Government procurement does not in any way obligate the U.S. Government. The fact that the Government formulated or supplied the drawings, specifications, or other data does not license the holder or any other person or corporation; or convey any rights or permission to manufacture, use, or sell any patented invention that may relate to them.

This report was cleared for public release by the Air Force Research Laboratory Rome Research Site Public Affairs Office and is available to the general public, including foreign nationals. Copies may be obtained from the Defense Technical Information Center (DTIC) (http://www.dtic.mil).

AFRL-SN-RS-TR-2007-102 HAS BEEN REVIEWED AND IS APPROVED FOR PUBLICATION IN ACCORDANCE WITH ASSIGNED DISTRIBUTION STATEMENT.

FOR THE DIRECTOR:

/s/	/s/
JAMES R. HUNTER Work Unit Manager	RICHARD G. SHAUGHNESSY Chief, Rome Operations Site Sensors Directorate

This report is published in the interest of scientific and technical information exchange, and its publication does not constitute the Government's approval or disapproval of its ideas or findings.

REPORT DOCUMENTATION PAGE

Form Approved
OMB No. 0704-0188

1. REPORT DATE *(DD-MM-YYYY)*	2. REPORT TYPE	3. DATES COVERED *(From - To)*
APR 2007	Final	Apr 05 – Mar 07

4. TITLE AND SUBTITLE

NON-ELECTRONIC RADIO FRONT-END (NERF)

5a. CONTRACT NUMBER

5b. GRANT NUMBER
FA8750-05-1-0101

5c. PROGRAM ELEMENT NUMBER

6. AUTHOR(S)

Bahram Jalali

5d. PROJECT NUMBER
N584

5e. TASK NUMBER
SN

5f. WORK UNIT NUMBER
02

7. PERFORMING ORGANIZATION NAME(S) AND ADDRESS(ES)
University of California
10920 Wilshire Blvd 1200
Los Angeles CA 90024-6523

8. PERFORMING ORGANIZATION REPORT NUMBER

9. SPONSORING/MONITORING AGENCY NAME(S) AND ADDRESS(ES)

Defense Advanced Research Projects Agency
3701 North Fairfax Dr.
Arlington VA 22203-1714

AFRL/SNDP
25 Electronic Pky
Rome NY 13441-4515

10. SPONSOR/MONITOR'S ACRONYM(S)

11. SPONSORING/MONITORING AGENCY REPORT NUMBER
AFRL-SN-RS-TR-2007-102

12. DISTRIBUTION AVAILABILITY STATEMENT
APPROVED FOR PUBLIC RELEASE; DISTRIBUTION UNLIMITED. PA# 07-146

13. SUPPLEMENTARY NOTES

14. ABSTRACT

Radio frequency (RF) communication systems are particularly vulnerable because the antenna provides a direct port of entry for electromagnetic radiation. This report describes a new type of RF receiver front-end that features a complete absence of electronic circuitry and metal interconnects – the traditional "soft spots" of a conventional RF receiver. The device consists of a dielectric resonator antenna that concentrates and feeds the signal onto a resonant electro-optic field sensor. The absence of metallic interconnects and the charge isolation provided by the optics removes the "soft spots" in a traditional receiver. In the proof-of-concept experiment, detection of C band electromagnetic signals at 7.38 GHz with a sensitivity of 4.3×10^{-3} V/m·Hz$^{1/2}$ is demonstrated. The dielectric approach has an added benefit: it reduces physical size of the front end – an important benefit in mobile applications.

15. SUBJECT TERMS

Dielectric resonator antenna, photonically isolated antenna receiver, electro-optic dielectric antenna, EMP isolated antenna

16. SECURITY CLASSIFICATION OF:			17. LIMITATION OF ABSTRACT	18. NUMBER OF PAGES	19a. NAME OF RESPONSIBLE PERSON
a. REPORT	b. ABSTRACT	c. THIS PAGE			James R. Hunter
U	U	U	UL	14	19b. TELEPHONE NUMBER (*Include area code*)

TABLE OF CONTENTS

LIST OF FIGURES

Summary

The threats to civil society posed by high power electromagnetic weapons are viewed as a grim but real possibility in the post September 11 world [1,2,3]. These weapons produce a power surge capable of destroying or damaging sensitive circuitry in electronic systems. Unfortunately, the trend toward reduced geometry and voltage renders modern electronics highly susceptible to such damage. Radio frequency (RF) communication systems are particularly vulnerable because the antenna provides a direct port of entry for electromagnetic radiation. Here we report a new type of RF receiver front-end that features a complete absence of electronic circuitry and metal interconnects, the traditional "soft spots" of a conventional RF receiver. The device consists of a dielectric resonator antenna that concentrates and feeds the signal onto a resonant electro-optic field sensor. The absence of metal interconnects and the charge isolation provided by the optics removes the "soft spots" in a traditional receiver. In the proof-of-concept experiment, detection of C band electromagnetic signal at 7.38 GHz with a sensitivity of 4.3×10^{-3} V/m·Hz ^{½} is demonstrated. The dielectric approach has an added benefit: it reduces physical size of the front end – an important benefit in mobile applications.

Introduction

The Graham Commission report, made to U.S. Congress' House Armed Services Committee on July 22, 2004, concluded that "high-altitude nuclear electromagnetic pulse (HEMP) is one of the few threats that can hold at risk the continued existence of civil society in the United States… The current vulnerability of our critical infrastructures can both invite and reward attack if not corrected" [3]. HEPM and other types of high power microwave weapons can shut down telecommunications networks without leaving behind a trace of the attacker [2]. They generate bursts of electromagnetic energy strong enough to damage or destroy electronic circuitry. Ironically, the danger is exacerbated by the impact of the celebrated Moore's law, which describes the electronic industry's relentless pursuit of miniaturization. The scaling has resulted in a continuing decrease in the maximum voltage that such circuits can tolerate, rendering modern electronics highly susceptible to damage from high power electromagnetic sources; for instance, voltages as low as 10 volts can punch through the gate oxide of a modern CMOS transistor. This value should be compared to the capabilities of HPM weapons, which can deliver transient potentials of tens of kilovolts inside a circuit. Catastrophic damage also results from melting and arcing of metallic interconnects by the large current surge produced by an HPM source [2]. Even less intense bursts can permanently damage circuits causing them to fail at a later time [2].

Optical FSR = Antenna center frequency	**10 GHz**
Field enhancement factor (β)	**25**
Dielectric constant of dielectric material	**38**
Dielectric constant of lithium niobate	**35**
EO resonator finesse (F)	**100**
Photodiode responsivity (R)	**0.8**
EO coefficient of lithium niobate, r_{33}	**30.8 pm/V**
Optical wavelength	**1.55 μm**
Antenna aperture (A_e)	**10^{-4} m^2**
Diameter of the lithium niobate disk resonator	**4.4 mm**
Refractive index of lithium niobate resonator (n_e)	**2.14**

Table 1 | Parameters for the RF sensitivity calculation.

Though most components in a system can be protected using Faraday cages, the front-end components in a communication system are particularly vulnerable because the antenna provides a direct path for electromagnetic pulse to enter the system. The conventional method for protecting circuits against high transient voltages utilizes a shunt diode to limit the voltage, but this method is best suited for lower frequencies [4]. At high frequencies (>5 GHz), the addition of the diode capacitance to the input node of the low noise amplifier will compromise the bandwidth and noise performance of the receiver. While steady incremental progress is being made in applying this technique to high frequency circuits, the fundamental and intrinsic limitation due to loading of the amplifier's input node remains. Because of the weak signal levels and sensitive electronics (the low noise amplifier) the receiver is more vulnerable and more difficult to protect than the transmitter in an RF front end. Presently, there are few options for protecting high frequency receivers from high power electromagnetic radiation. The proposed All-Dielectric Non-Electronic (ADNERF) radio front-end technology is aimed at addressing this need.

Methods, Assumptions, and Procedures

The vulnerability to high power microwaves can be mitigated by eliminating all metallic components and transistors in the RF front end, and by providing charge isolation between the front-end and down stream electronic data-processing circuitry. We create such a device by combining a dielectric antenna with a sensitive optical field sensor. Fig. 1 shows a conceptual description of this photonic-assisted all-dielectric RF front-end technology. The dielectric antenna is a leaky resonator that is fabricated from a material with low loss and high relative permittivity. The incoming signal in the form of free space electromagnetic field excites a

resonance mode of the antenna resulting in a desired build up of field inside the structure. We exploit this enhanced electric field to modulate an optical carrier in a linear electro-optic crystal. To enhance the receiver sensitivity, the crystal is formed into a resonator (a microdisk in present case). An optical waveguide, such as a single mode fiber, transfers the signal to the system back-end where a photodetector converts it to an electrical signal that is subsequently processed using conventional electronics.

The novelty behind this new technology is multifold. First, the antenna itself is made of only dielectric materials. With no metallic electrodes and interconnects present in the front-end, the high field damage caused by arcing or melting of metallic components is eliminated. Second, the subsequent electrical-optical-electrical conversion provides charge isolation. Our device exploits this function in a similar spirit to an optocoupler – a common device that creates electrical isolation between two nodes of a low-speed digital circuit (by using an LED and a photodetector to create a short optical link between them). However, there are critical differences between the optocoupler and the new technology we present here. The traditional optocoupler uses semiconductor devices, metallic interconnects and electrodes. Furthermore, its utility is limited to the situations where a standard digital logic signals are used. The device lacks the high frequency response and the sensitivity that is required in an analog RF receiver. The third advantage of the proposed device originates from the fact that the dielectric antenna is made of high permittivity materials and is smaller than the conventional metallic antennas, resulting in a highly compact front-end. In fact, antenna size reduction is the main motivation for use of dielectric antennas in conventional applications [5, 6, 7].

We choose a cylindrical geometry for the dielectric resonant antenna (DRA) and perform the design using finite element simulations carried out with the High-Frequency Structure Simulator (HFSSTM). The optimum location for the electrooptic crystal is the position inside the DRA where the maximum RF field enhancement occurs. One of the objectives of finite element simulations is to identify this location, which in turn depends on the resonant mode of the DRA. The design reported here takes advantage of the TM011+δ mode of the DRA because it provides a high electric field on the top and bottom cylinder surfaces with field lines that are perpendicular to these surfaces. The electrooptic crystal can then be placed outside the cylinder as shown. While this geometry is not the optimum in terms of receiver sensitivity, it eliminates the need to embed the crystal inside the DRA. This simplifies device packaging, facilitates the proof of concept demonstration, and is the main motivation for our choice of the cylindrical DRA design. The DRA material we used is a composite ceramic (BaTiO3 based) with relative permittivity $\varepsilon_r = 38$ and a loss tangent of 0.0005 at microwave frequencies. The dimensions are fine-tuned (11.25 mm in diameter, 9 mm high) to give $TM_{011+\delta}$ resonance at 7.38 GHz, which matches the free spectral range of the optical resonator (reason will be explained later). Fig. 1b shows the electric field pattern when the DRA is excited by a 7.38 GHz plane wave incident from the broadside. The field enhancement factor (β), defined as the ratio of DRA resonant field strength to the free space field, is approximately 18. This quantity impacts the receiver sensitivity as described later.

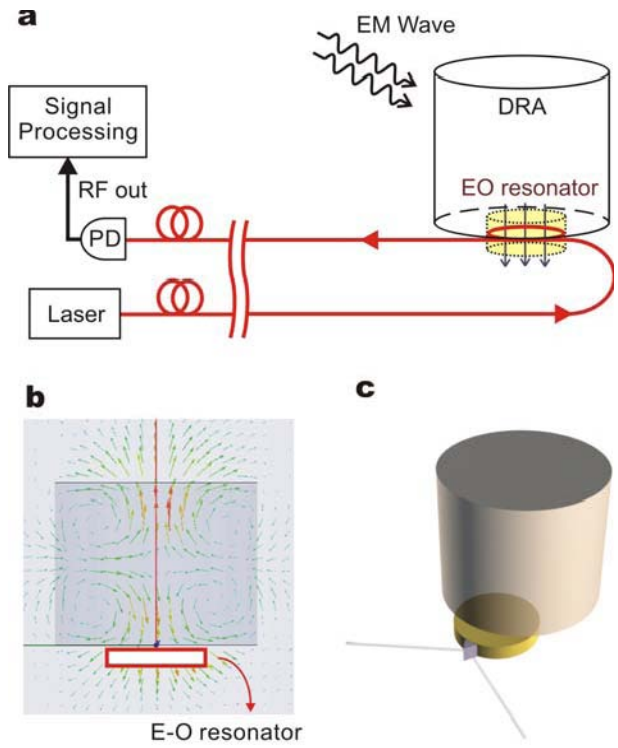

Figure 1 Photonic assisted all-dielectric RF front-end technology.

a. The concept of the photonic assisted all-dielectric RF front-end technology. An electrooptic empowered dielectric antenna captures the free space RF signal. The embedded optical link provides complete electrical isolation between the air interface and electronic circuitry that only appear after photodetector. b. Numerical simulation of the distribution of electric field inside a cylindrical DRA (11.25 mm in diameter, 9 mm high). c. 3D drawing of the DRA integrated with a electrooptic microdisk resonator.

The E-O microdisk resonator is fabricated from commercially available z-cut $LiNbO_3$ substrates. The c-axis is normal to the disk and optical resonance is achieved by confining a TE-polarized optical field in a high-Q whisper-gallery mode (WGM) along the periphery of the disk [6], [7]. Fig. 2 shows the transmission spectrum of the $LiNbO_3$ resonator. The measured loaded quality factor is $Q \sim 1.1\times10^6$, corresponding to a bandwidth of 175 MHz at 1.55 μm. Adjacent resonance peaks are separated by free spectral range (FSR) which is 7.38 GHz in this case. Because of the long photon lifetime in the high-Q $LiNbO_3$ resonator, optical waves interact with the electric field on multiple passes, which increases the total phase shift. In this configuration, even a small electric field applied across the disk is enough to induce a shift in the WGM resonance frequency with a magnitude comparable to its bandwidth. As a result, receiver sensitivity is enhanced.

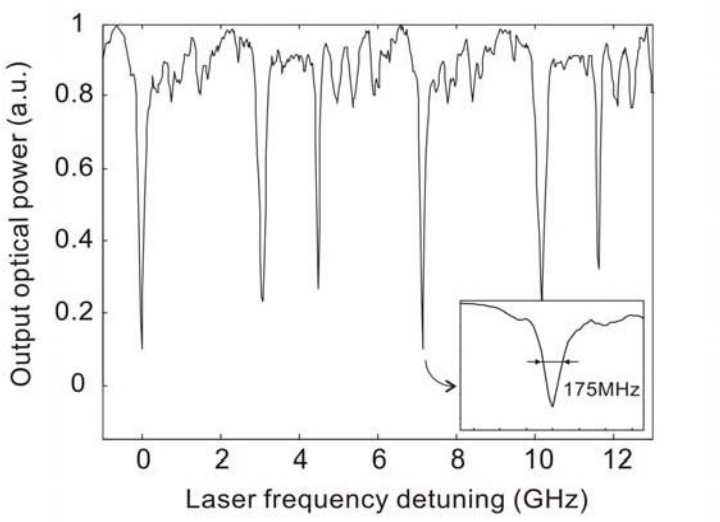

Figure 2 Optical resonance spectrum of the electrooptic ($LiNbO_3$) microdisk. Optical transmittance spectrum of TE whisper-gallery modes in $LiNbO_3$ microdisk resonator; diameter = 5.9mm, FSR = 7.38GHz, Q~1.1×10^6

When the input laser frequency (f_0) is tuned to a particular optical resonance mode, high frequency modulation can be achieved if the modulation sidebands reside in adjacent optical resonance modes, i.e., when the modulation frequency (f_m) is equal to the optical FSR [11,12], as shown in Fig. 3**.** If the E-O resonator is critically coupled, the maximum slope point occurs when the laser is tuned to about 25% of peak transmission. However, the modulating E-field (E_{RF}) must not be uniform across the disk otherwise no modulation sidebands will be created [11,12]. Optimal modulation efficiency happens when $L_{eff} = 2\pi r/2$, where L_{eff} is the length over which the modulating E-field and the optical wave overlap. To approximate this condition, the E-O resonator is placed off center from the symmetrical axis of DRA (Fig. 1c).

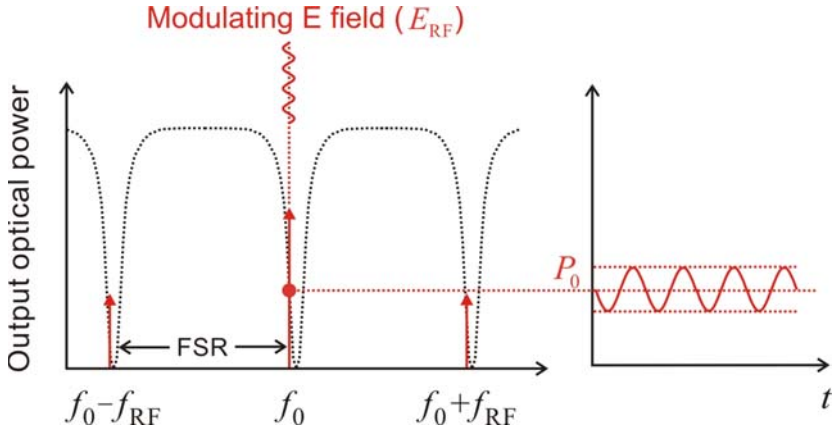

Figure 3 E-O Modulation.

High speed electro-optic modulation is possible when the optical FSR matches the RF carrier frequency (f_{RF})

An analytical expression for the sensitivity of our receiver is obtained by finding the free space RF power that results in a unity carrier to noise ratio (CNR) at the photodetector. The result is:

$$P_{\mathrm{m,min}} = \left(\frac{E_{\mathrm{m,min}}}{\beta} \frac{\varepsilon_{\mathrm{LN}}}{\varepsilon_{\mathrm{DRA}}} \right)^2 \frac{A_{\mathrm{e}}}{\eta},$$

where A_e is the DRA cross-section, η is the impedance of free space (377 Ω) and ε_{DRA} and ε_{LN} are the dielectric constants of the DRA and $LiNbO_3$ at microwave frequencies, respectively. E_{min} is the minimum electric field that must be incident on the $LiNbO_3$ to achieve a CNR of unity and is given by:

$$E_{\mathrm{m,min}} = \frac{2\pi E_{\pi}}{9RP_0F} \sqrt{6\sigma_T^2},$$

where n_e is the extraordinary index of refraction at the operation wavelength, R is the photodetector responsivity, F is the finesse of the electrooptic resonator, P_0 is the average optical power and is the total variance of noise current, consisting of contributions from thermal noise, shot noise and the laser relative intensity noise (RIN). The half wave field E_π is defined as,

$$E_{\pi} = \lambda / (n_e^3 r_{33} L_{eff})$$

where λ is the optical wavelength and r_{33} is the electrooptic coefficient. Fig. 4 indicates typical RF sensitivities that our receiver can achieve. The parameters used for these calculations is described in Table 1. As an example, an RF sensitivity of -150dBm/Hz can be achieved using a common DFB laser that produces an average power of 10mW and has a relative intensity noise (RIN) of -150dB. This is roughly 10dB better than the requirements of a WiFi receiver (IEEE 802.11a). The performance can be further improved with DRA optimization.

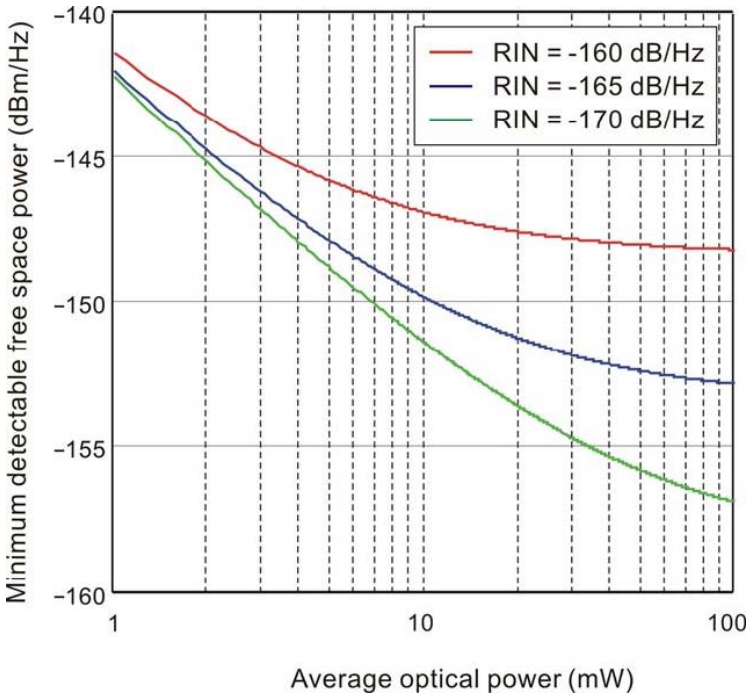

Figure 4 Receiver sensitivity.

Calculated receiver sensitivity versus average optical power incident on the photodetector. A constant laser RIN noise was assumed. The sensitivity is a strong function of laser power and RIN noise level. The model used for sensitivity calculations is described in the Methods section.

Results and Discussion

To experimentally demonstrate the new device, we used a setup similar to that shown in Fig. 1a**.** Light from an external cavity tunable laser was coupled to a microdisk resonator using a diamond prism. A horn antenna illuminates the receiver with a 7.38 GHz RF signal. A photodetector module with a built-in transimpedance amplifier (New Focus 1544A) performs opto-electronic conversion. The received signal was analyzed on an RF spectrum analyzer. The detector had a manufacturer-specified optical noise equivalent power of NEP = 33 $pW/Hz^{1/2}$, a responsivity of 0.6 A/W and a transimpedance gain of 1000 V/A. This corresponds to an output RF noise level of -140 dBm/Hz generated by the detector. It also has a specified saturation power of 1 mW. In all our experiments, the optical power incident on the photodetector was 0.5 mW in order to stay below the 1 mW saturation limit of the photodetector. The noise and saturation limit of the detector severely limited the sensitivity that our prototype RF receiver could achieve in the experiments. The overall receiver had a bandwidth (-3 dB) of 35 MHz, determined primarily by the RF resonance within the DRA.

Fig. 5 shows the received signal spectrum with and without the dielectric antenna. As the DRA is removed away from the $LiNbO_3$ crystal, signal level decreases by 50 dB. The RF spectrum analyzer's resolution bandwidth was set to 100Hz. The observed noise floor of -140 dBm/Hz (-120 dBm over 100 Hz instrument bandwidth) is generated by the amplified photodetector as explained above. Fig. 6 shows the received RF power versus the free space power incident on the dielectric antenna. The latter was obtained by calculating the fraction of the power fed into the

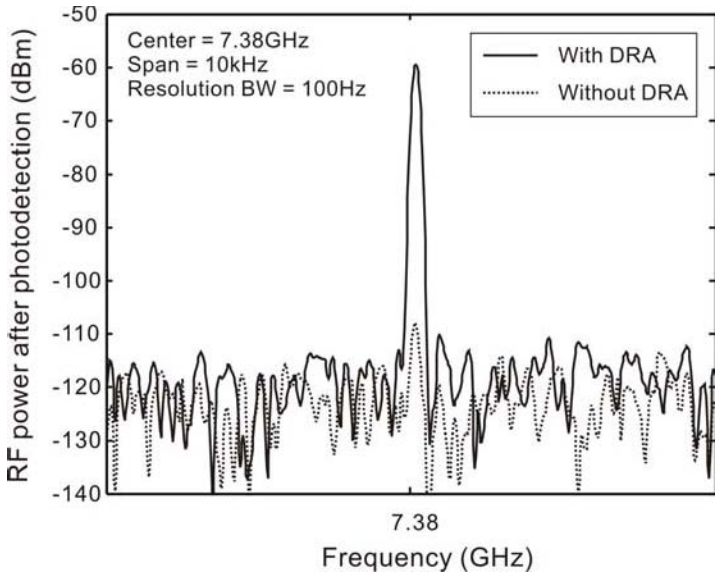

Figure 5 Detection of free space RF signal by the prototype receiver. Response to the 7.38 GHz EM wave transmitted by horn antenna with (solid line) and without (dashed line) the DRA in the front-end. The 16 dBm of power was fed into the horn antenna. This noise floor is limited by the noise produced by the amplified photodetector module.

horn antenna that falls onto the dielectric antenna using a standard model for the radiation pattern of the horn antenna [8]. The minimum detectable free space RF power is -63 dBm or equivalently -83 dBm/Hz. This corresponds to a minimum detectable electric field = 4.3×10^{-3} V/m $Hz^{½}$ and is limited by the noise of the detector. The maximum RF power applied to the horn antenna was limited to 16 dBm by the available RF source.

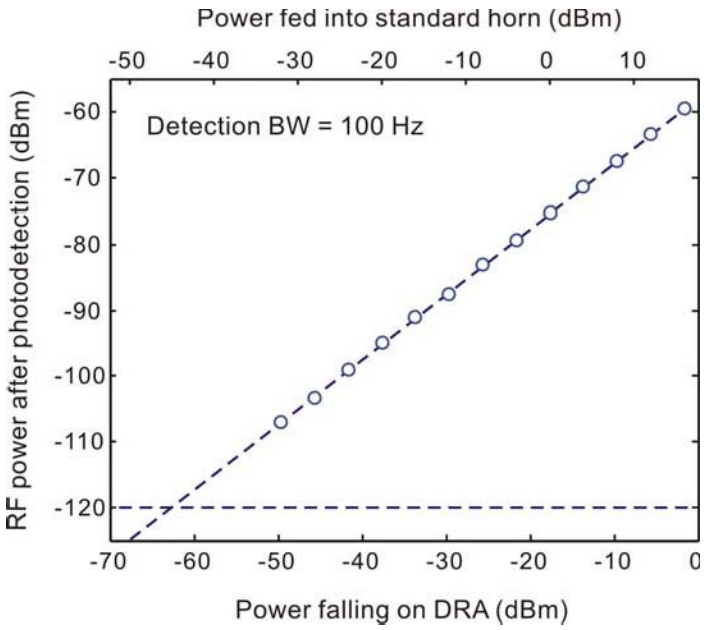

Figure 6 Measured transfer characteristics of the prototype receiver.
The response of the photonic-assisted all-dielectric RF receiver with resolution bandwidth of the RF spectrum analyzer set to 100 Hz.

Achieving better performance as predicted in Fig. 4 will require a better photodetector which has a lower noise performance and higher saturation power. Furthermore, for ease of integration, the $LiNbO_3$ resonator was placed outside the DRA. For optimum performance the $LiNbO_3$ resonator can be integrated within the DRA where the maximum electric field resides.

A comment about the high field immunity of the proposed device is called for. The dielectric strengths of DRA and $LiNbO_3$ materials are about 10^5 V/cm [9-10], similar to those in common semiconductors and dielectrics used in integrated circuit manufacturing. However, in a typical integrated circuit, voltage surge appears across the gate insulator of the front-end transistor, which is on the order of 100 nm or less in a high speed transistor. In the dielectric antenna, this dimension is on the order of the free space RF wavelength divided by the square root of the dielectric constant, which leads to a value of about 6 mm (10 GHz signal and a dielectric constant

of 36). Even with a field enhancement factor of 20 (18 in the prototype device) the electric field inside the DRA (and the $LiNbO_3$) will be a factor of 10^3-10^4 lower than that occurring in the front-end transistor.

Conclusion

We have reported a new type of RF receiver that features absolutely no metal electrodes, interconnects and transistors in the front end. The novel All-Dielectric Non-Electronic Radio Front-end (ADNERF) receiver can be realized by using a dielectric resonator antenna in conjunction with a resonant electro-optic field sensor. By eliminating the soft-spots of a conventional receiver, the new technology is aimed at addressing the vulnerability of today's wireless communication and radar systems.

References

[1] Special Issue on High-Power Electromagnetics (HPEM) and Intentional Electromagnetic Interference (IEMI), *IEEE Trans. EMC* **46**, (2004).

[2] Abrams, M. Dawn of the e-bomb. *IEEE Spectrum* **40**, 24-30 (2003).

[3] Report of the Commission to Assess the Threat to the United States from Electromagnetic Pulse (EMP) Attack, Volume 1: Executive Report 2004, http://www.globalsecurity.org/wmd/library/congress/2004_r/04-07-22emp.pdf

[4] Gong, K., Feng, H., Zhan, R. & Wang, A. Z. H. A Study of Parasitic Effects of ESD Protection on RF ICs. *IEEE Trans. on Microwave Theory and Tech.* **50**, 393-402 (2002).

[5] Dettmer, R. Dielectric Antenna Make Waves. *IEE Review* **49**, 28-31 (2003).

[6] Petosa, A., Ittipiboon, A., Antar, Y. M. M., Roscoe, D. & Cuhaci, M. Recent advances in dielectric resonator antenna technology. *IEEE Trans. Antennas Propagat.* **40**, 35-48 (1998).

[7] Long, S. A., McAllister, M. & Shen, L. C. The Resonant Cylindrical Dielectric Cavity Antenna. *IEEE Trans. Antennas Propagat.* **31**, 406-412 (1983).

[8] IEEE Standard Methods for Measuring Electromagnetic Field Strength of Sinusoidal Continuous Waves *IEEE Std 291-1991*

[9] S. Panteny, R. Stevens, and C. R. Bowen, "Characterisation and Modelling of Barium Titanate-Silver Composites," Integrated Ferroelectrics, 63: 131–135, 2004, pp. 131-135.

[10] Theodor Tamir, *Guided-Wave Optoelectronics*. Berlin Heidelberg: Spring-Verlag, 1988.

[11] Ilchenko, V. S., Savchenkov, A. A., Matsko, A. B & Maleki, L. Sub-MicroWatt Photonic Microwave Receiver. *IEEE Photon. Technol. Lett.* **14**, 1602-1604 (2002).

[12] Cohen, D. A., Houssein-Zadeh, M. & Levi, A. F. J. Microphotonic modulator for a microwave receiver. *Electron. Lett.* **37**, 300-301 (2001).